Supporting Information

Giardina et al. 10.1073/pnas.1111456108

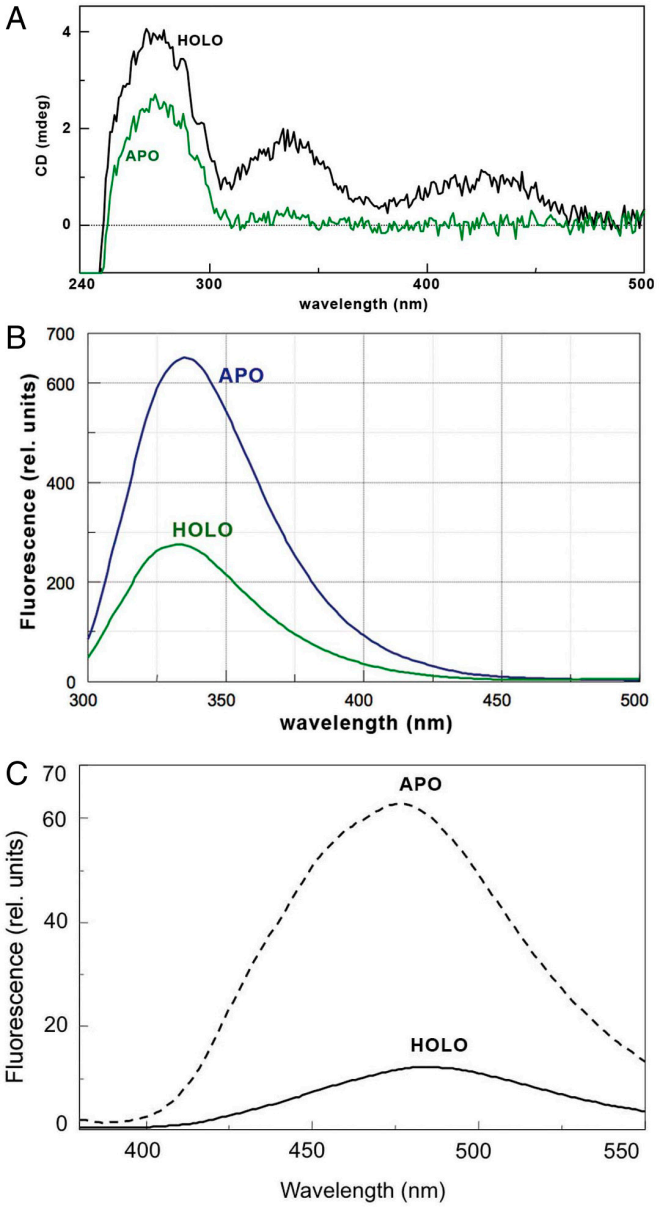

Fig. S1. Near-UV CD spectra, intrinsic and ANS fluorescence spectra of holo and apo-hDDC. (*A*). Near-UV and Vis CD spectra of 5 μM holo (*Black*) and apoenzyme (*Green*). (*B*). Fluorescence emission spectra of 1 μM holo (*Green*) and apoenzyme (*Blue*). Excitation at 280 nm (*C*). Fluorescence emission spectra of 1 μM holo (–) and apoenzyme (- - -) incubated in the presence of 15 μM 8-Anilino-1-naphthalenesulfonate (ANS) at 25 °C for 1 h, registered upon excitation at 365 nm. All measurement were made in 0.1M Potassium Phosphate buffer pH = 7.4.

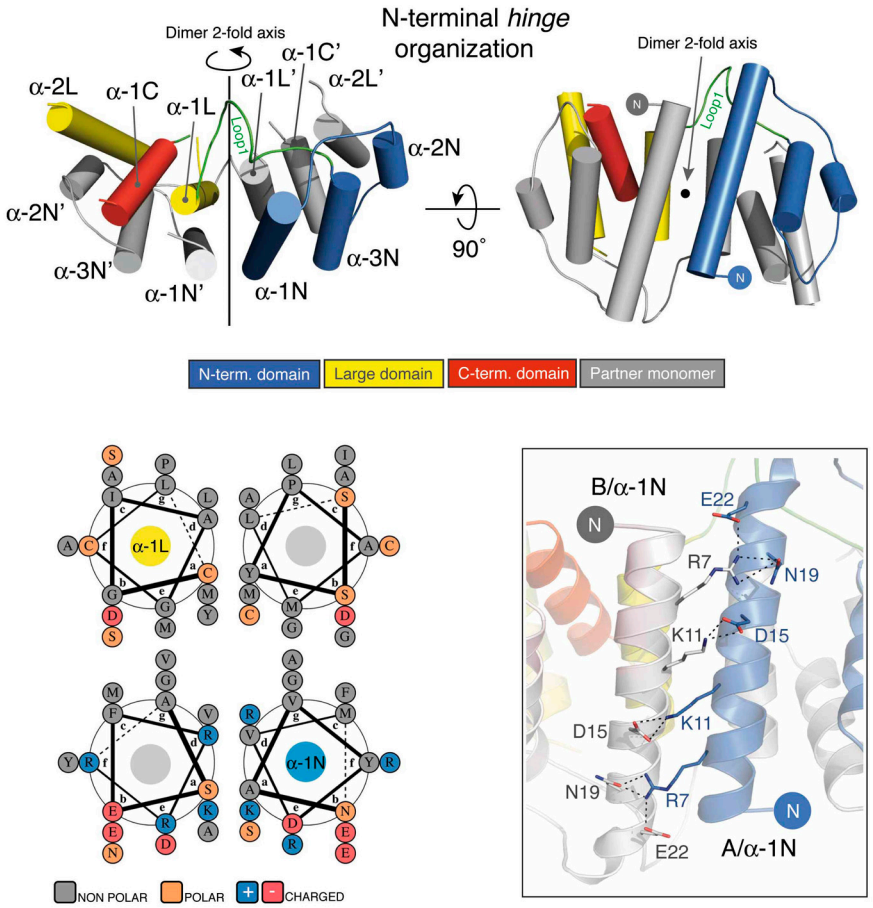

Fig. S2. Structural organization of the N-terminal hinge (the dimer interface). Organization of the 12 helices cluster that arises from the domain swapping of the N-terminal domain which is peculiar of the Group II decarboxylases. These helices are organized as an extended four helix bundle network and build the dimer interface; i.e., the hinge of the bivalve shell (see Fig. 1). Color code: *Blue*—N-terminal domain; *Yellow*—Large domain; *Red*—Small domain; residues that are not part of the interface were removed for clarity. The capital letters used after the helix number denote the domain to which each helix belongs (i.e., α-1N—N-terminal, α-1L—Large, α-1C—C-terminal). The lower part of the figure shows a helical-wheel diagram and a cartoon representation of the central four helix bundle (α-1N − α-1L + α-1N′ − α-1L′) illustrating the strong hydrophobic interaction of the core and the network of hydrogen bonds of the surface residues.

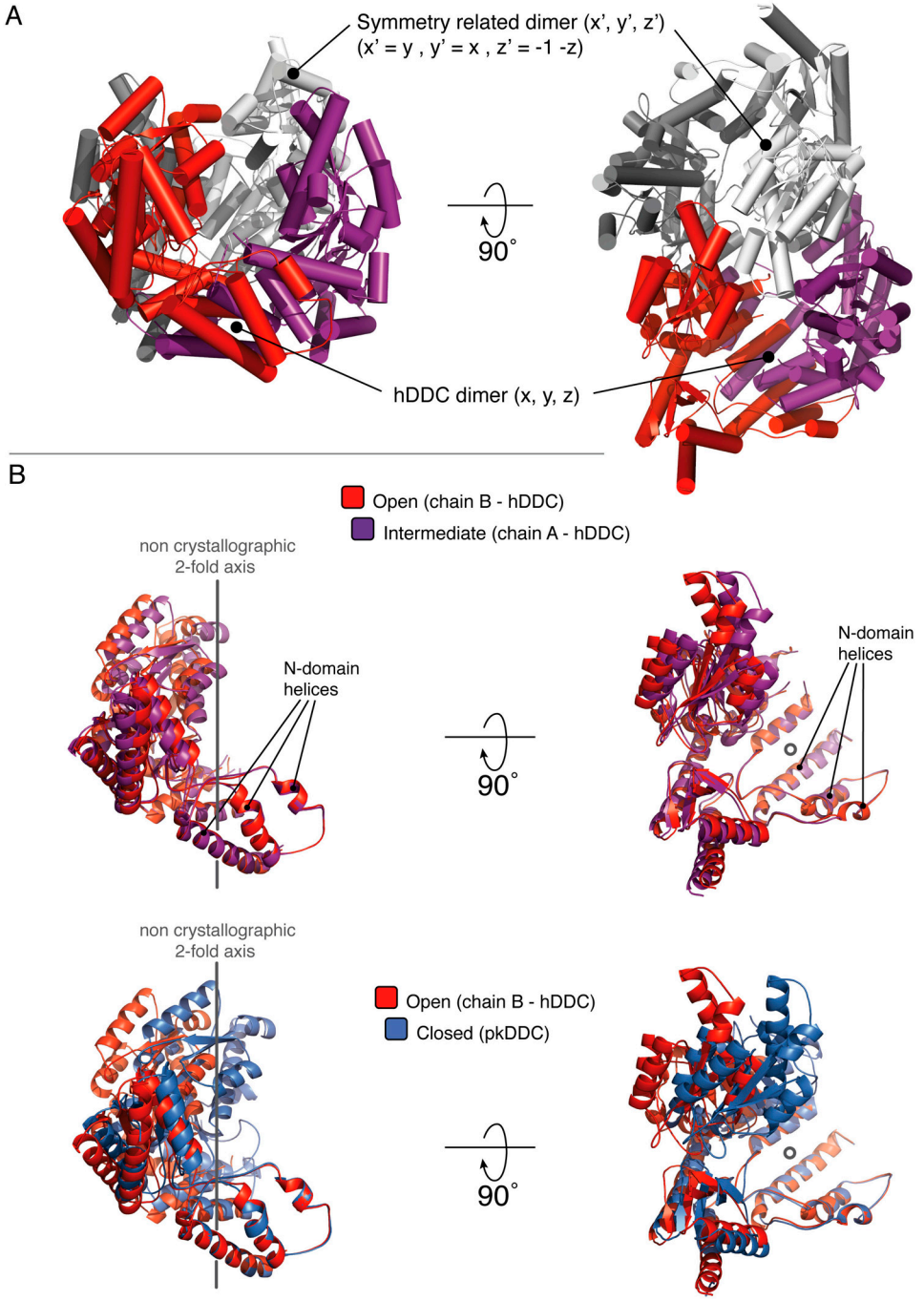

Fig. S3. Intermolecular crystal contacts and asymmetry of the two dimer subunits. (*A*). Tetrameric assembly of hDDC in the crystal lattice. Each dimer in the open conformation *bites* a symmetry related mate, corresponding to the equivalent position *y*, *x*, *-z* of an adjacent cell. The space group is $P4_12_12$. (*B*). Top—Superposition of the two monomers of hDDC on the N-domain helices (*Red*: chain-B; *Purple*: chain-A) reveals that the structure of the two subunits is not symmetrical, with chain-A being more closed than chain-B. The monomers are shown in the same orientation as in (*A*). *Bottom*—superposition, on the N-domain helices, of the open monomer (chain-B) of hDDC (*Red*) with the pkDDC (pdb id: 1JS6) closed monomer (*Blue*). Open, Intermediate and Closed refer to the different conformations of the monomer as illustrated in Fig. 2.

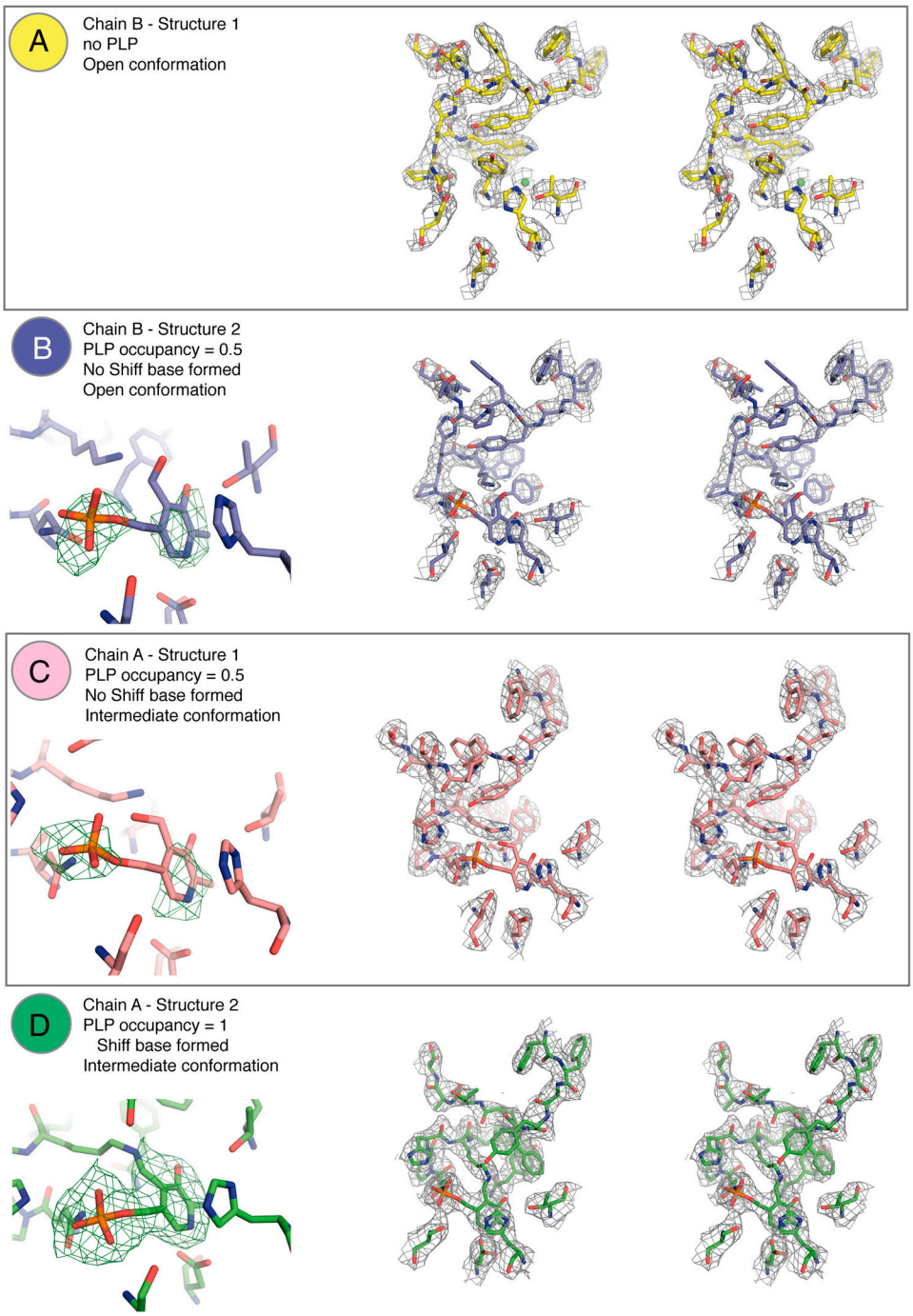

Fig. S4. Electron density of the alternative conformations of the active site. On the *left*: Fo-Fc omit map calculated for PLP and contoured at 2.0σ. On the *right*: Stereo representation of the 2Fo-Fc map contoured at 1.3σ.

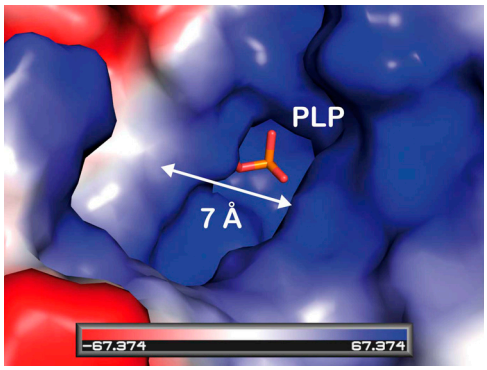

Fig. S5. Access to the active site in the closed pkDDC dimer. Surface representation colored by electrostatic potential of the active site access in the closed conformation (pkDDC—pdb id: 1js6). Only the phosphate group of the cofactor is visible inside the 7 Å wide gorge.

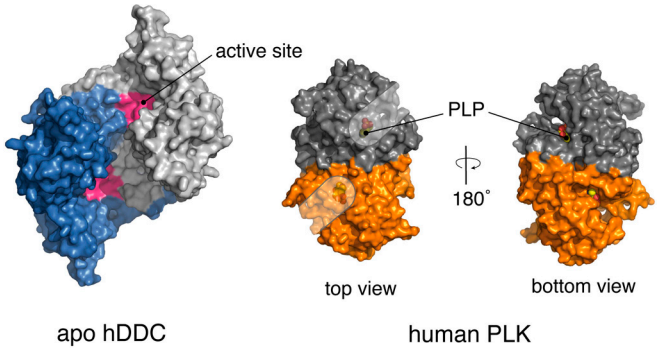

Fig. S6. Structural complementarity between the PL Kinase (PLK) dimer and the open apo-hDDC. On the *left*, a top view of the open apo-hDDC dimer showing the position of the exposed active sites (*magenta*); on the *right*, top and bottom views of the human PLK dimer (pdb id: 3keu). The transparency in the top view illustrates the position of the PLP and the direction of the access channels to the substrate binding site, which are visible in the bottom view. In a possible complex between the two proteins the two PLP molecules bound to PLK would face exactly the active sites of DDC.

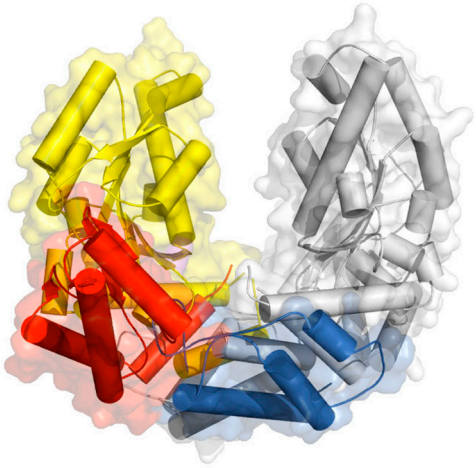

Movie S1. Domain organization of the apo hDDC dimer. The first part of the animation shows the Tertiary and Quaternary structure of the apo-hDDC dimer in the open conformation. The second part illustrates the organization of the dimer's hinge; the domain swapping of the N-domains.

Movie S1 (MOV)

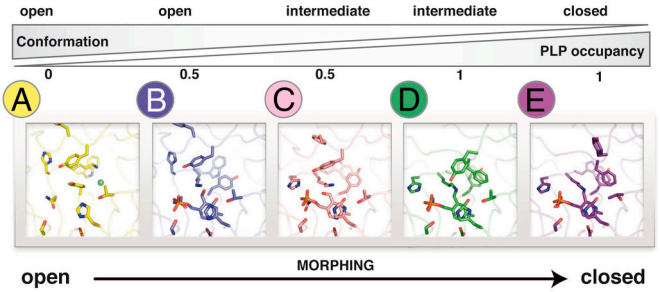

Movie S2. Five step morphing through the alternative conformations of the active site of DDC. The animations is a five step morphing through the different conformations of the active site of DDC as ordered in Fig. 2. Letters corresponding to the five different states appear (top left corner) each time the morphing corresponds to a crystal structure. Notice that morphing is a simple animation from the starting coordinates to the ending coordinates. No kinetic, thermodynamic or molecular dynamic calculation is employed.

Movie S2 (MOV)

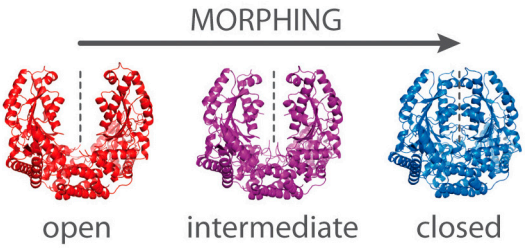

Movie S3. Morphing through the different monomer conformations of DDC. The animation shows the morphing from an hypothetical symmetric dimer with both monomers in the open conformation (*Red*) to the closed conformation (*Blue*—pkDDC structure), passing through the intermediate conformation (*Purple*). The second part of the movie focuses on the conformational transition of loop1, after PLP binding, followed by folding of the mobile loop2 and loop3 residues, which are structured only in the closed conformation. Notice that during the animation, for technical reasons, PLP is not morphing together with the protein and its position, in the starting and ending points, is shown only for clarity. Notice that morphing is a simple animation from the starting coordinates to the ending coordinates. No kinetic, thermodynamic or molecular dynamic calculation is employed.

Movie S3 (MOV)

Table S1. List of 23 point mutation of DDC identified in patients with various neurotransmitters disorders. The mutations are taken from BIOMDB database (http://www.biopku.org/BioPKU_databasesBIOMDB.asp). Mutants which are part or make direct interaction with the structural determinants involved in the conformational change discussed in the paper are highlighted. A brief description of their role or nature of the interaction is also provided

Mutation	Position	Interaction	Type of interaction (conformation)
Y79C	Loop1		swapping position with F80 going from the apo to the holo state
H72Y	Loop1		adjacent to W71 (see Fig. 4)
T69M	Loop1		same as above
H70T	Loop1		same as above
R462P		Loop1	H-bond with Y75 (open)
R447H		Loop1	H-bond with the C = O of Y79 (closed)
E25K		Loop1	interacting with Y75 (closed)
L408I		Loop1	interacting with F80 (closed)
G102S	Loop2		involved in substrate binding
A110Q	Loop2		
F309L		Loop2 Loop3	involved in substrate binding; contacts both Loop2 and Loop3 residues in the closed structure; it is mobile in the open structure
R347Q	Loop3		involved in substrate binding
R358H	Loop3		H-bond with D310 of the catalytic Loop (open)
R7X	N-ter. Hinge (α-1N)		H-bond with N19 and E22 (see Fig. 2)
A91V	N-ter. Hinge (α-1L)		hydrophobic core of the central 4-helix bundle
L38P	N-ter. Hinge (α-2N)		disruption of α-2N
P47H			
S147R			
S250F			
A275T			
R285W			
V460G			
R412W			

Table S2. Data collection and refinement statistics for structure 1–3 (see Fig. 2)

	Structure 1	Structure 2	Structure 3
Coordinates	3RBF	3RCH	3RBL
Data collection *			
Beamline	BESSY (BL-1)	ESRF (ID14-1)	ESRF (ID14-1)
Space group	$P4_12_12$	$P4_12_12$	$P4_12_12$
Cell dimensions			
$a = b,c$ (Å)	175.84, 74.96	177.00, 74.83	179.64, 74.95
Resolution (Å)	2.90 (3.06–2.90)	2.80 (2.95–2.80)	3.25 (3.40–3.25)
R_{sym} or R_{merge}	11.2 (47.9)	13.3 (61.2)	13.1 (40.1)
$I/\sigma I$	15.7 (3.6)	13.6 (3.5)	13.8 (3.8)
Completeness (%)	99.3 (99.3)	100 (100)	99.8 (100)
Redundancy	8.8 (6.0)	7.1 (7.2)	6.4 (6.2)
Refinement			
Resolution (Å)	45.0–2.9	30.0–2.8	30.0–3.25
No. reflections	26,369	28,290	18,961
R_{work}/R_{free}	21.2/26.6	20.1/25.9	22.1/28.3
No. atoms			
Protein (chain A/B)	3,474/3,480	3,504/3,461	3,469/3,480
PLP (chain A/B)	16/–	15/16	
Ion	2		1
Water		28	
Mean B-factor (Å^2)			
Protein (chain A/B)	18.1/18.2	25.9/26.2	48.0/45.3
PLP (chain A/B)	35.2/–	34.8/34.9	
Ion	40.1		56.4
Water		16.8	
rmsd			
Bond lengths (Å)	0.011	0.011	0.011
Bond angles (°)	1.263	1.318	1.301
Ramachandran: n. residues (%)			
favored	710 (90.7)	699 (89.7)	721 (92.2)
allowed	71 (9.1)	78 (10.0)	60 (7.7)
disallowed	2 (0.3)	2 (0.3)	1 (0.1)
Molprobity scores (percentile)	2.62 (89th)	2.94 (69th)	2.83 (91st)

*Values in parentheses are for highest-resolution shell.